Composite Structures, Volume 297, October 2022, Article number 115972
DOI:10.1016/j.compstruct.2022.115972

Filament Wound Pipes Optimization Platform Development: A Methodological Approach

Roham Rafiee*,[1], Reza Shahzadi[1], Soheil Jafari[2]

[1]*Composites Research Laboratory, Faculty of New Science and Technologies, University of Tehran, Tehran 1439955171 Iran*

[2] *Centre for Propulsion Engineering, School of Aerospace Transport and Manufacturing (SATM), Cranfield University, Bedford MK43 0AL, UK*

Abstract -A multi-objective and multi-level optimization procedure is developed for obtaining optimal structural design of filament wound composite pipes in oil and gas industries. At the first stage, regulated design constraints are identified. Required computational tools for predicting structural properties of the composite pipes are developed and validated through experimental study. Then, the pipe design procedure is formulated as an engineering optimization problem where a hybrid design-optimization platform is developed to deal with that. The platform integrates multi-objective genetic algorithm on level 1 with a premutation-based direct search approach on level 2. It is aimed to minimize the cost of the pipe while maximum values for other structural properties are expected. Manufacturing limitations are also taken into account as the constraints in addition to design requirements.

Keywords: *Composite pipes; Genetic algorithm; Experimental validation; Computational modeling; Filament winding*

* Corresponding author's email: Roham.Rafiee@ut.ac.ir

List of symbols

Symbol	Description	Symbol	Description
ρ_A^C	Areal density of the cross layer	ρ_A^H	Areal density of the hoop layer
ρ_{FRP}	density of composites	ρ_f	Fiber density
ρ_m	Resin (matrix) density	W_f	fiber weight fraction
V_m	Resin volume fraction	V_f	Fiber volume fraction
N_S	number of fiber strands in the fiber bundle	B	band width of the fiber bundle
t_{Hoop}	Thickness of a hoop layer	t_{Cross}	Thickness of a cross layer (including two balanced angle plies)
p	Number of hoop plies	q	Number of cross plies
t_r	Thickness of structural layers (w/o liner)	D_i	Internal diameter
θ	Winding angle	T	Tex (mass of fiber per one km of fiber length)
HTS	Hoop tensile strength of pipe	LTS	Longitudinal (axial) tensile strength of pipe
PS	Pipe stiffness	E_H	Hoop modulus of a layer
$\bar{I}$	centroidal moment of inertia of the cross-sectional area of the wall per unit length	Y	
NA	location of neutral axis	E_H^{pipe}	Hoop modulus of the pipe structure
P_c	External failure pressure	E_A^{pipe}	Axial modulus of the pipe structure
P_N	Nominal pressure	P_F	Internal failure pressure
σ_u	Axial elastic buckling stress	SF	Safety factor
E_f	Fiber modulus	E_m	Matrix modulus
G_f	Shear modulus of fiber	G_m	Shear modulus of resin
ν_f	Poisson's ratio of fiber	ν_m	Poisson's ratio of resin
X_T	Longitudinal tensile strength of a ply	X_C	Longitudinal compressive strength of a ply
Y_T	Transverse tensile strength of a ply	Y_C	Transverse compressive strength of a ply
S	In-plane shear strength of a ply	X_f	Tensile strength of fiber
X_m	Tensile strength of matrix	X'_m	Compressive strength of matrix
S_m	Shear strength of resin	E_X	Longitudinal modulus of a lamina
E_Y	Transverse modulus of a lamina	E_S	In-plane shear modulus of a lamina
ν_x	Major Poisson's ratio of a lamina	X_f	Tensile strength of fiber
C_{SL}	Correction factor for long-term stiffness	C_{PL}	Correction factor for long-term pressure

1. Introduction

Optimization plays an essential role for the engineering design of composite structures in the modern era. As the main requirement for surviving in the marketplace, the industrial sectors are required to present the safe products with competitive price.

Weight reduction, increasing the strength and enhancing the durability accompanied with the reduced final cost of products are the main constraints in design procedure of various structures. Nowadays, the wide spectrum of industrial segments exploits composite materials because of their high strength/stiffness to weight

ratio. Composite materials can potentially enhance the mechanical performance of the products in comparison with their traditional counterparts. The final cost of the manufactured components from composites is dominantly governed by the material consumption. Optimal design architecture of composite structures can noticeably prevent excessive consumption of raw materials mainly rooted in over-designed products. Finding the best solution from both mechanical and economical points of view is accomplished through optimization procedure.

Fiber-Reinforced Plastic (FRP) pipes are widely used in the infrastructure of countries for conveying water, waste-water, petrochemical fluids, oil and gas, because of their unique characteristics. The cost of installation, repair and maintenance for FRP piping systems are less expensive than that of other traditional ones. Therefore, the final price of the produced FRP pipes is the key element in defining the final cost of the piping systems. Utilizing FRP pipes with proper mechanical performance while keeping the price at the lowest possible level have always been desired in cost-effective pipelines. This target can be achieved through optimal structural design of FRP pipes.

In the open literature, considerable efforts have been done to characterize the mechanical response of FRP pipes/vessels under various loading [1]. In contrast, limited studies have been devoted to the case of minimizing the final cost of the FRP pipes through optimal structural design.

Jin et al. [2] proposed a safety evaluation method based on the strength and fracture characteristics of pipe wall materials and suggested a formula to calculate an optimum pipe wall thickness for a pipe undergoing live and dead loads. Almeida Jr. et al. [3] proposed a genetic algorithm (GA) for the optimization of the stacking sequence to improve strength of a cylindrical shell under internal pressure with and without manufacturing restrictions. Minsch et al. [4] have analyzed different aspects of filament winding process and equipment technology and derived a decision matrix for process engineering for improving the selection of proper equipment for a particular design. Two methodologies for optimization of a type III pressure vessel were proposed by Alcantar et al. [5] where weight minimization was the objective function. A useful analytical tool was provided by Colombo and Vergani [6] for the optimal design of a composite pipe minimizing the wall thickness taking into account internal pressure and axial loads. The influences of stacking sequence and fiber orientation on energy absorption in cylindrical composites were studied by Zhang et al. [7] and optimal ply angle were obtained based on finite element modeling and analysis. Liu and Shi [8] have established a model to calculate the winding-induced residual stresses in thick cylinders undergoing internal pressure and

performed optimization to maximize the failure pressure. The optimal fiber orientation is extracted for FRP vessels under hydrostatic pressure through genetic algorithm targeting minimum weight and maximum buckling load by Hajmohammad and his co-workers [9].

The main motivation of this research is the previous studies conducted by the first author and his co-workers on developing various methods for analyzing mechanical performance of FRP pipes from different aspects during the last 10 years [10-34]. It has been clearly revealed that some constraints are in contradiction. For instance, structural designers of FRP pipes adjust fiber orientation to obtain proper structural performance. Due to inherent anisotropic behavior of FRP pipes, their longitudinal tensile strength (LTS) is generally different from circumferential tensile strength referred to as hoop tensile strength (HTS). Thus, increasing angle of fiber orientation from pipe axial direction to circumferential direction is resulted in higher HTS whilst LTS is reduced. Furthermore, the level of material consumption in helically wound layers are much more than hoop layers. Therefore, the optimum combination of hoop and helical layers with proper winding angles are required to be extracted. This has been usually carried out through the old scenario of trial and error by industrial centers relying on the knowledge of designer experts. Therefore, the importance of optimizing structural design of FRP pipes becomes much more pronounced.

2. Problem statement

The main objective of this article is to develop a procedure for optimal structural design of FRP pipes satisfying design constraints regulated by normative standards and minimizing the final cost. The FRP pipes are intended to be used in gas network. Classified as the constraints of optimization problem, all design requirements dictated by normative standards and also manufacturing limitations are firstly identified. Then as the second stage, proper computational procedures for estimating the structural properties of FRP pipes are developed and validated. Treating design architecture of composite layers as design variables, a multi-objective and multi-level optimization scenario is developed. The overall roadmap of the study is shown in Fig. 1 and details of each step are elaborated in preceding sections.

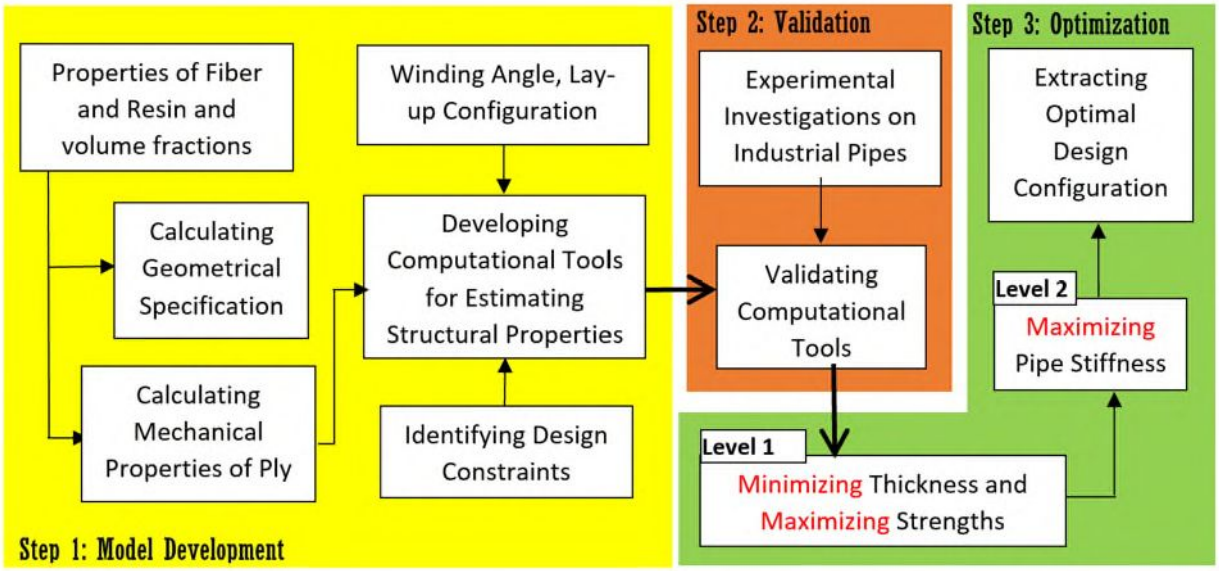

Fig. 1: Roadmap of the study

3. Computational methods

It is intended to optimize the structural design of FRP pipes for the application field of petroleum and natural gas industries. Thus, design constraints are identified in accordance with ISO 14692 [35]. It is worth mentioning that just those design constraints related to the structural design of the FRP pipes are taken into account here. Other constraints which have not been affected by structural design are not covered here, like fire performance, static electricity and resistance against corrosion.

Computational methods used for estimating identified constraints of the FRP pipes are presented. The optimization scenario is in need of efficient computational tools for predicting the constraints based on the structural design which are accurate enough and also rapid.

3.1. HTS and LTS

The ultimate strength of the FRP pipe along circumferential (hoop) or axial (longitudinal) directions are hereinafter referred to as HTS and LTS, respectively. Since, the structural design of FRP pipes for the purpose of petroleum and gas applications demands more accurate computational tools in comparison with water/waste-water application, progressive damage modeling (PDM) is used for predicting HTS and LTS. The flowchart of the PDM utilized in this research is presented in Fig. 2. The procedure consists of model preparation, stress analysis, failure evaluation and material degradation. At the model preparation stage, lay-up configuration, loadings and material properties are provided. LTS of the FRP pipe is measured on flat

specimen cut along the axial direction of the pipe and subjected to tensile loading [36]. For measuring the HTS of the pipe, a ring specimen is cut from the pipe and then split-disk experiment is performed [37]. Thus, the applied loading to both LTS and HTS specimens are also shown in Fig. 2. These loadings are considered at the stage of model preparation. The stress analysis is performed using classical lamination theory (CLT) [38] and failure is evaluated based on Hashin failure criteria [39]. For the purpose of runtime consideration, the degradation of mechanical properties are accomplished through ply-discount method [40]. Readers are referred to reference [34] for detailed information about this method, since the development of the utilized PDM is beyond the scope of this study. Hashin failure criteria and also degradation rules are provided in Appendix A.

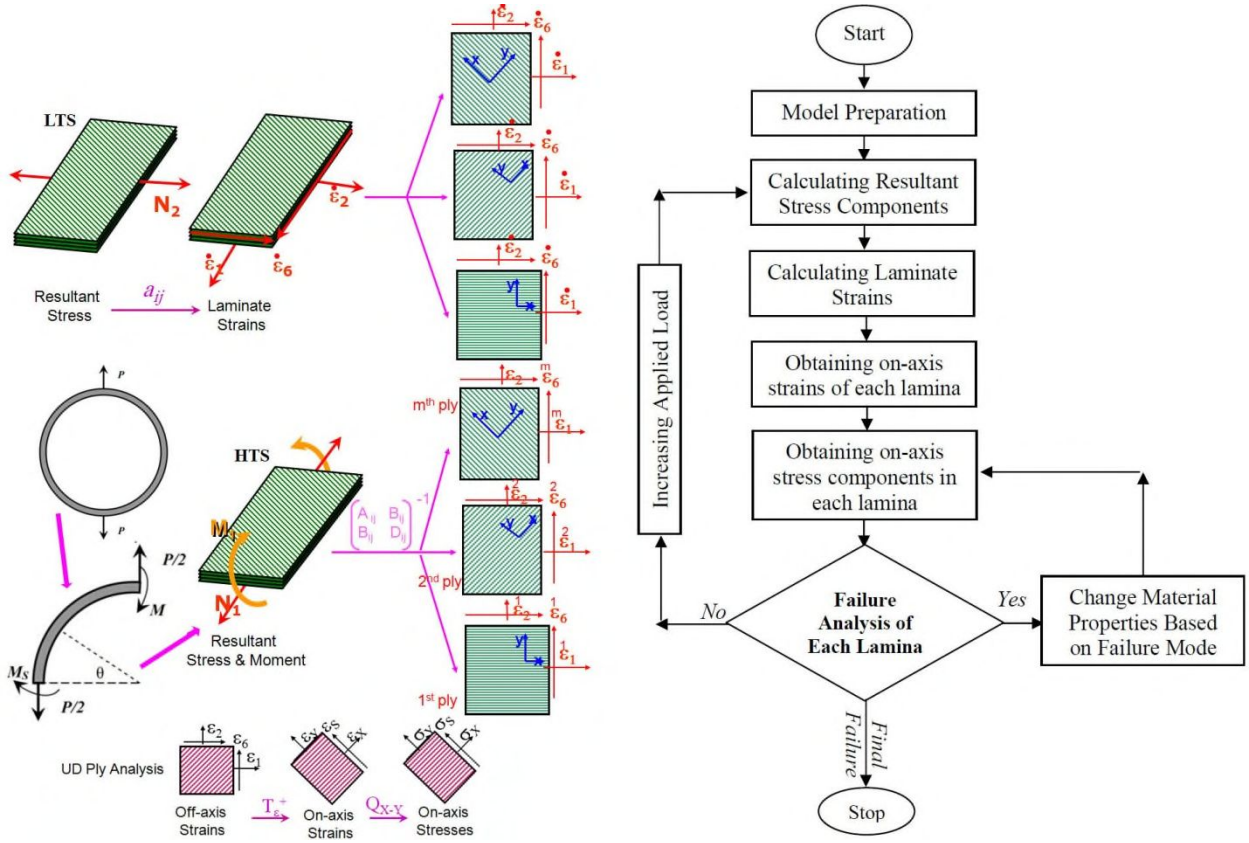

Fig. 2: Flowchart of PDM for obtaining LTS and HTS

3.2. Failure pressure

The failure pressure is defined as the maximum pressure where either structural failure or functional failure occurs. Structural failure, known also as burst failure, implies on the ultimate limit loading pressure. But functional failure is identified in the form of leakage wherein an internal fluid finds a path through-the-thickness of the FRP pipes. Although the functionally failed pipe can still accommodate loadings from structural point of view, it cannot practically sustain its mission. The functional failure pressure is less than the

burst pressure. In this research, functional failure is considered as the failure pressure PDM is also utilized in this section for estimating the failure pressure with slight difference with the PDM technique presented in the preceding section. If all layers of the pipe experience matrix cracking and/or shearing failure, it is considered as functional failure and thus the associated pressure is reported as failure pressure. The flowchart of the PDM utilized for the purpose of estimating failure pressure is presented in Fig. 3.

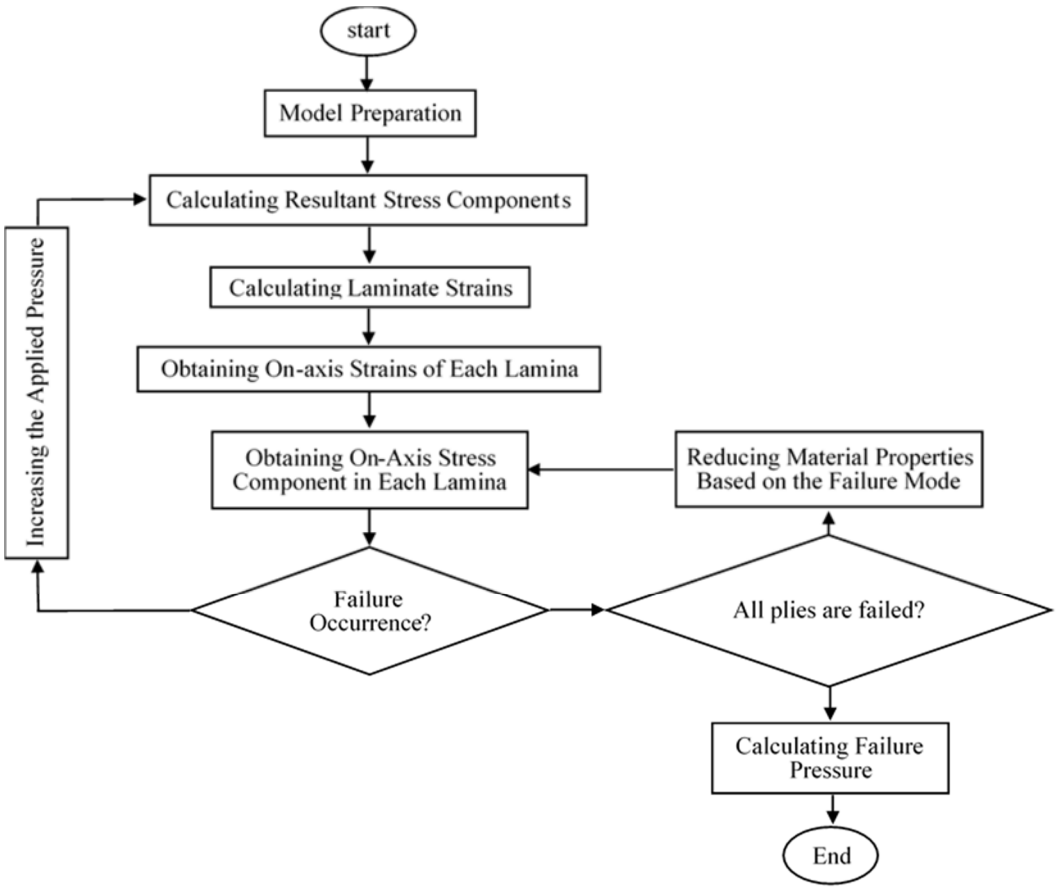

Fig. 3: Flowchart of PDM for predicting failure pressure

3.3. Pipe stiffness

Indicating the resistance of the pipe against external transverse loading, pipe stiffness is an important parameter especially for underground applications. Subjected to transverse loading due to the dead or traffic loadings, the circular cross section of the pipe is deformed into an oval shape. The experienced ovality has a negative side effect on the fluid transmission from hydraulic point of view. Moreover, oval deflection of the pipe cross-section is resulted in decreasing its second moment of area. Therefore, higher level of stress than perfect circular cross sections is induced as another negative effect on the mechanical integrity of the pipeline. The pipe stiffness is generally expressed using below formulation [21]:

$$\frac{E\bar{I}}{D^3} = PS \tag{1}$$

The stiffness of FRP pipes as a structural property can be tailored by its structural design. Considering FRP pipes as layered structures, the Eq. (1) is reformed as below [21]:

$$PS = \frac{\sum_{i=1}^{last\ ply} E_H^i \bar{I}^i}{(D_i + 2NA)^3} \tag{2}$$

where reflected parameters in Eq. (2) are calculated as below [21]:

$$E_H = \frac{1}{\frac{m^4}{E_x} + \frac{n^4}{E_y} + \frac{m^2 n^2}{E_s} - \frac{2\nu_x m^2 n^2}{E_x}} \quad , \quad m = cos\theta, n = sin\theta \tag{3}$$

$$NA = \frac{\sum_{i=1}^{last\ ply} E_H^i t^i \bar{Y}^i}{\sum_{i=1}^{last\ ply} E_H^i t^i} \tag{4}$$

$$\bar{Y}^i = \frac{t^i}{2} + \sum_{m=1}^{i-1} t^m \tag{5}$$

As it is clear from Eqs. (2) to (5), the lay-up sequence is important in estimating pipe stiffness.

The procedures for calculating thickness and mechanical properties are reflected in Appendix B.

3.4. External pressure

External pressure can cause transversal buckling in pipe [41]. The external pressure causing failure in a pipe can be estimated using below formulation [35]:

$$P_c = 2(\frac{1}{SF})E_H^{pipe}(\frac{t}{D})^3 \tag{6}$$

the safety factor is taken as 1.5 when the pipe is exposed to short-time vacuum and it is considered as 3 if the pipe is expected to be exposed to long-term vacuum [35]. After obtaining hoop modulus of each layer through Eq. (3), the hoop modulus of pipe is obtained using CLT [38].

3.5. Axial buckling (shell buckling)

The axial elastic buckling stress for a cylinder in pure bending is calculated as [35]:

$$\sigma_u = 0.9 \times \beta \frac{E_{eff} t_r}{D} \tag{7}$$

where:

$$E_{eff} = \sqrt{E_A^{pipe} E_H^{pipe}} \tag{8}$$

$$\beta = 0.1887 + 0.8113 \frac{0.83}{\sqrt{0.1 + 0.005(D_i/t_r)}} \tag{9}$$

4. Validation of computational methods

Before performing optimization procedure, the developed computational tools for estimating structural properties of FRP pipes are required to be validated. Consequently, different FRP pipes are manufactured using reciprocal filament winding techniques. Then HTS, LTS, failure pressure and pipe stiffness are measured using tensile test [36], split-disk experiment [37], hydrostatic test [42] and parallel plate loading [43], respectively. All four experimental procedures are shown in Fig. 4.

Fig. 4: Measuring Failure pressure, HTS, LTS and pipe stiffness (left to right)

Mechanical properties of the utilized fiber and resin are presented in Appendix C. The volume fractions of constituents are also measured through procedure *G* of ASTM D3171 [44] and obtained values are used as input data in corresponding Eqs. reflected under Appendices A and B. The bandwidth of fiber bundle was adjusted at 180 mm containing 42 strands.

Since it is impractical to measure the thickness of cross and hoop plies, separately, total thicknesses of all pipes are measured. An excellent agreement was observed between computed and measured thicknesses. The outputs of the developed computational tools are compared with experimental observations in Tables 1 to 3.

Table 1: Comparing estimated HTS and LTS with experimental observations

DN [mm]	Lay-up	LTS [N/mm]		HTS [N/mm]	
		PDM (Error)	Experimental	PDM (Error)	Experimental
300	$[90/\pm60.2_2/90]$	140.12 (2.58%)	143.83	1468.24 (1.95%)	1497.44
300	$[90_2/\pm60.2_5/90_3]$	353.12 (2.23%)	361.17	3750.44 (2.47%)	3845.54
500	$[90_2/\pm57.5_4/90]$	273.07 (4.42%)	285.69	2180.34 (2.23%)	2230.2
500	$[90_2/\pm60.2_6/90_3]$	387.04 (5.49%)	409.54	3935.1 (2.37%)	4030.55
600	$[90_2/\pm60.2_4/90_2]$	253.55 (5.4%)	268.19	2771 (2.41%)	2840.18

As it can be seen from Table 1, the discrepancy between the results of estimating either LTS or HTS through PDM with experimental observations fall below 6%. Thus, the PDM technique can efficiently be used for predicting HTS and LTS of FRP pipes.

Table 2: Comparing estimated stiffness with experimental observations

DN [mm]	Lay-up	Stiffness (Pa)	
		Solid mechanic method (Error)	Experimental
300	$[90/\pm60.2_2/90]$	2569 (8.3%)	2800.6
400	$[90/\pm60.2_3/90_3]$	2499 (10%)	2775
500	$[90_2/\pm57.5_4/90]$	4171 (8.2%)	4546.4
600	$[90_2/\pm60.2_4/90_2]$	2091 (7.4%)	2258.3
700	$[90_2/\pm52.5_5/90_3]$	2756 (9.1%)	3031.6

The results of Table 2 imply on the proper accuracy of the solid mechanic method for predicting stiffness. Thus, the simple method of solid mechanic based on cross-sectional analysis of built-up beam is adequate for predicting pipe stiffness in this research. The underestimated stiffness through solid mechanic model can be viewed as a benefit for the optimization scenario, since unreliable design configurations will be prevented.

Table 3: Comparing failure pressure with experimental observations

DN [mm]	Lay-up	Failure Pressure (MPa)	
		PDM (Error)	Experimental
300	[90/±60.2/90]	6.11 (8.91%)	5.61
300	[90/±60.2]	4.33 (7.71%)	4.02
400	[90/±60.2]	3.34 (9.51%)	3.05
700	$[90/\pm52.5_3]$	2.42 (3.2%)	2.5

The results of Table 3 also shows that proposed PDM method for predicting failure pressure presents acceptable accuracy, despite the slight overestimation. As it can be seen from the reported results in Table 3, almost in all cases PDM overestimate the failure pressure. This can be attributed to different sources like neglecting stress concentration in failed plies, neglecting the curvature of the pipe and/or assuming linear behavior. It should be pointed out that this shortcoming will be overcome by defining a correction factor which will be explained in proceeding section.

5. Optimization framework

The FRP pipes is categorized by three parameters as DN-PN-SN, where DN is internal diameter, PN is nominal pressure and SN is nominal pipe stiffness. The main objective is to optimize the structural design of FRP pipes with any combination of DN-PN-SN character where the final cost is minimum. As another objective, it is also intended chose a design configuration leading to the maximum values for all HTS, LTS and PS. Thus, the optimization problem is a multi-objective problem.

The minimum requirements of HTS and LTS are reflected in normative standards based on the nominal DN and PN of the pipe [35]. Specifically, for LTS, two different categories are regulated in relative standards [35] known as open-end or closed-end pipes. Similar to pressure vessels, the minimum value of LTS should be half of the HTS in closed-end pipes; while for open-end pipes the minimum LTS is much less than the half of HTS. In contrast with open-end condition, the pipes are required to resist longitudinal load produced by the internal pressure in end closure condition. Moreover, higher values of LTS associated with closed-end condition are also very suitable for the purpose of pipe-jacking because of applied axial loading during installation. The pipe stiffness should be also equal to or greater than nominal SN. The soundness of each FRP pipe is evaluated

through the hydrostatic test with twice the nominal pressure for duration of 30 seconds [35]. Therefore, the failure pressure should be more than the twice the nominal pressure by default.

The ratio of the buckling stress to the maximum axial stress shall be greater than 3 [35]. Since the maximum axial stress of the pipe cannot exceed LTS, thus axial elastic buckling (σ_u) should be equal to or greater than three times the LTS.

Moreover, FRP pipes for the application fields of oil and gas are required to sustain their mission till 20 years [35]. The qualification of the FRP pipes for long-term service is approved through a series of long-term examinations. The long-term behaviors of the pipe from both pressure and stiffness class are characterized on the scale of 10,000 hours. The results are extrapolated to 20 years and the remaining pressure/stiffness is evaluated. Consequently, two additional constraints are taken into account to address long-term pressure and stiffness.

Any optimization procedure is regulated by the objective(s), constraints and variables. For the purpose of this study, aforementioned parameters are presented in Table 4.

Table 4: Formulation of design procedure as an engineering optimization problem

Objectives and Levels	**L1**: Minimizing total wall thickness (Eq. (B7)) **L1**: Maximizing HTS **L1**: Maximizing LTS **L2**: Maximizing PS
Design Constraints	HTS ≥ values in [35] based on DN and PN LTS ≥ values in [35] based on DN, PN and end-condition (Open-end OR Closed-end) $\sigma_u \geq 3LTS_{netting}$ $P_c > 0.15$ *bar*
Manufacturing Constraints	θ = [50°, 70°] W_f = [73%, 77%]
Qualification Constraints	$P_F \geq 2.C_{PL}.PN$ $PS \geq C_{SL}.SN$
Design Variables	(i) No. of hoop layers (p) (ii) No. of cross layers (q) (iii) Winding angle (θ) in cross layers (v) Lay-up sequence
Input Parameters by User	DN-PN-SN

	Mechanical properties of fiber and resin C_{PL} and C_{SL} End-load condition (Open-end OR Closed-end)

The objective function for the optimization problem is detailed in Table 4 where the wall thickness (Eq. (B7)) will be minimized in level 1; while maximizing HTS and LTS. The pipe stiffness (PS) will be maximized in level 2 (the optimization procedure is illustrated in Fig. 5). To take the real-world considerations into account, design, manufacturing, and qualification constraints are also added to the objective function as presented in Table 4. HTS/LTS and failure pressure are estimated through the introduced PDM procedures under sections (3.1) and (3.2), respectively. Pipe stiffness is also calculated based on the presented formulation under section (3.3).

As it can be seen from Table 4, the nominal pressure entered by user is enhanced by some correction factors. This strategy not only cover the qualification requirements of the pipe, but also overcome any probable overestimation of failure pressure through PDM (section 3.2).

Rafiee and Ghorbanhosseini have done experimental and theoretical study on long-term stiffness and found out that initial stiffness will reduce about 30% after 20 years [12, 15, 16]. Thus, C_{SL} is considered as 1.2 in this research. C_{PL} is also assumed as 1.1 based on the simulation performed for long-term hydrostatic test [27, 28]. It is worth mentioning that both C_{SL} and C_{PL} are required to be obtained through experimental tests for each pipe and suggested values in this research are provided for the purpose of conducting optimization scenario without loss of generality. Explicitly stated in normative standards, long-term experiments as qualification tests should be conducted to approve the structural design of FRP pipes.

Changing the lay-up sequence by keeping the same lay-up configuration will change the pipe stiffness, whilst other calculated constrains (i.e., HTS, LTS, P_c and P_F) will stay unchanged. Therefore, the optimization is implemented on two levels. At the first level, all constraints except pipe stiffness (PS) are required to be satisfied and possible design configurations are extracted accordingly. Consequently, the output populations of the first level of optimization are divided into two groups. The first group contains those design patterns whose calculated stiffness values fulfill the requirements of that constraint. The second group cover those design configurations whose stiffness are less than the minimum requirements. At the second level, all possible permutations for lay-up sequence of the second group are considered. Among them, those cases fulfilling the

requirements of the stiffness are chosen. Finally, among all realized alternatives, the optimum case with maximum stiffness is identified. The overview of the optimization scenario in this research is shown in Fig. 5.

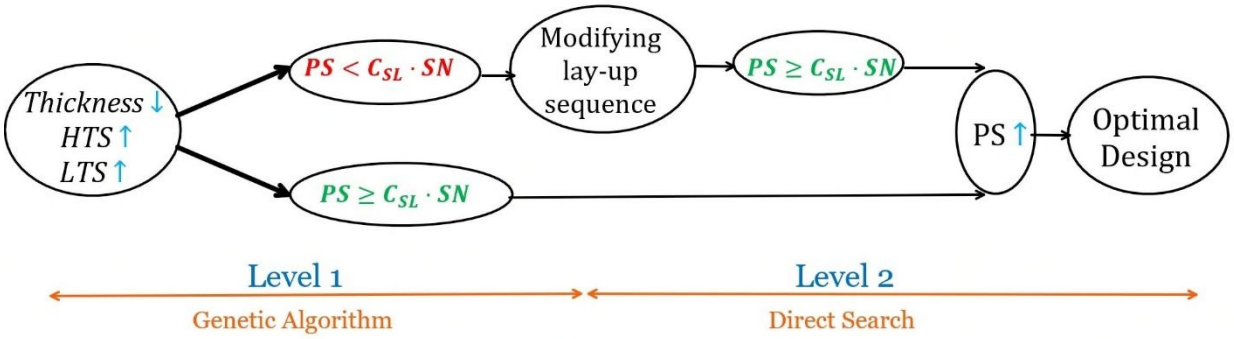

Fig. 5: Overview of optimization levels

As an effective means for dealing with practical problems, Global optimization (GO) algorithms are being widely used in real-world engineering problems with respect to their flexibility and model independent nature [45-49]. To explore the solution space thoroughly, the first level of optimization is conducted by utilizing the Genetic Algorithm (GA) due to interminable number of potential solutions. The second level is carried out by utilizing a premutation-based direct search to exploit the area where the GA has converged to. As there are multiple conflicting objectives to optimize (Thickness, LTS, and HTS), the Multi-Objective (MO) feature of the GA is being used based on the concept of Pareto-set and solution ranking developed by Fonseca and Fleming [50,51] to achieve the Pareto-front for the problem. The precise formulation of the engineering optimization problem (Table 4) will satisfy the requirements of finding the Pareto-optimal as well as diversity of the found solutions [52]. An archive of solution with the best rank will be developed in the first level and will be permutated to find the best design. In the second phase, to assess all possible layer placement permutations, the concept of binary numbers is used to characterize the layer arrangement in which the number of digits of the binary number represents the total number of layers (p+q), the digits "1" represent the hoop layers and the digits "0" represent the cross-layers. Since there is no difference between two cross-layers or two hoop layers, the number of possible permutations to place the layers next to each other is $\frac{(p+q)!}{p!\times q!}$.

A computer code is developed on MatLab platform 2020b referred to as OPTICOPIPE®. OPTICOPIPE® has equipped with an interface where the user can target various objectives through various combinations for maximizing or minimizing LTS, HTS or PS besides minimum thickness. In this research, OPTICOPIPE® is

implemented for the aforementioned scenario in Table 4. The runtime of the OPTICOPIPE® on a computer with Core-i7 processor is less than one minute for each case.

The Multi-Objective Genetic Algorithm (MOGA) parameters are tuned based on the guidelines of Mauro Birattari in "Tuning Metaheuristics" [53] to get the optimal results. The reliability and repeatability criteria are also satisfied by running each case for 15 times. The computational effort for different cases varies from 115 seconds to 170 seconds (on an Intel(R) Core (TM) i7-6700HQ CPU@2.60GHz) which is not comparable with those of direct search method (in order of hours). Moreover, the population size, crossover fraction, and Pareto front population fraction are set as 50, 0.8, and 0.35 respectively.

The limitations of the current model can be summarized as extracting stress components through CLT, utilization of simple 2-D form of Hashin failure criteria and also simple linear solid mechanics theory for calculating pipe stiffness. Since, thin-walled pipes are investigated, application of CLT in combination with Hashin failure criteria can be considered as a rational compromise in the current modeling procedure which is also evident from the compatibility between experimentally measured values and theoretically estimated ones through Tables 1 to 3. Regarding the linear elastic theory for calculating pipe stiffness, large deformation phenomenon as the main source of non-linearity has not been taken into account. It has been shown that taking into account this issue through FEA will be led to the higher level of pipe stiffness a little [21]. Therefore, current method is slightly underestimating pipe stiffness rendering the model as the conservative one.

5. Results and discussion

Different pipe specifications are chosen as case studies and the optimization process is implemented for them to obtain their optimal design configurations. The outputs of optimization are presented in Table 5.

Table 5: Outputs of multi-objective optimization for structural design of FRP pipes

Pipe specification {DN-PN-SN}	End condition [O or C]*	t [mm]	Lay-up configuration	Fiber wt%	HTS [N/mm]	LTS [N/mm]	PS [Pa]
700-16-1250	O	6.4	$[90_3/\pm57.5_4/90_3]$	76%	3008	297	1651
	C	10.5	$[\pm50_{11}]$	77%	3383	1191	3782

400-32-7500	O	5.8	$[90_3/\pm52.5_4/90_3]$	77%	2895	389	9119
	C	11.4	$[\pm50_{12}]$	77%	3695	1301	25284
200-20-10000	O	3.5	$[90/\pm52.5_3/90]$	77%	1508	290	12348
			$[90/\pm55_3/90]$	76%	1538	252	12289
	C	4.2	$[90/\pm50_4]$	77%	1494	433	14048
500-16-2500	O	5.2	$[90_3/\pm62.5_4/90_2]$	76%	2914	220	3015
600-20-2500	O	7	$[90_2/\pm52.5_6/90_2]$	77%	3011	579	3738
450-18-1250	O	3.7	$[90_2/\pm55_3/90]$	77%	1836	258	1558
400-25-2750	O	4.2	$[90_2/\pm52.5_3/90_2]$	77%	2040	292	3340
375-25-4000	O	4.5	$[90_3/\pm55_3/90_2]$	77%	2368	259	5122
375-32-4000	O	4.8	$[90/\pm62.5_5/90]$	77%	2589	280	4896

*: O: Open-end, C: Closed-end

According to netting analysis, the best design configuration for the pipes with close-end condition from mechanical point of view is cross plies with winding angle close to 54.7º resembling pressure vessels [53]. But it can be seen from Table 4 the optimal winding angle is different in several cases, since other objectives like minimum thickness and maximum stiffness are also taken into account. For the specific case of {200-20-10000} pipe with close-end condition, the optimal design is the combination of a hoop and four cross layers when maximum HTS and minimum thickness are simultaneously sought. Exceptionally for {200-20-10000} pipe with open-end condition, two optimal designs are found with the same thickness wherein HTS is maximum in one case and LTS is maximum in another one. This is attributed to the intrinsically opposite behavior of HTS and LTS. The values of PS for the close-end cases are extremely higher than that of minimum design requirement, since the minimum admissible LTS for these cases are very high and thus more layers are required to be utilized.

As it is evident from the outputs, the optimal designs are associated with the higher values of fiber weight fraction, i.e., 76% or 77%. This is truly expected, because the higher values of weight fraction will be resulted in less thickness (Eqs. (B1) and (B5) in Appendix B). Therefore, OPTICOPIPE® is also powered with this feature to define the value of fiber weight fraction as an input parameter instead of a design variable at the beginning. This would be quite useful when the fiber weight fraction cannot be adjusted to its maximum due to the wet ability of utilized fiber. For instance, the optimal design configuration of {600-20-2500} is adjusted

from [$90_2/\pm52.5_6/90_2$] for fiber wt% of 77% to [$90_3/\pm52.5_4/90_3$] for the fiber wt% of 73% with 6.4-mm thickness.

The detailed results for one of the case studies of the Table 5, i.e. {600-20-2500}, is shown in Fig. 6 to confirm the effectiveness of the proposed approach as well as the validity of the design procedure formulation as an engineering optimization problem. The developed Pareto-front confirms the exploration capability of the algorithm while the average speed and the average distance between individuals confirm the ability of the algorithm in exploitation of the solution space. The rank and score histogram assess convergence to the Pareto-front [55]. Stopping criteria is set as either time limit or number of generations (100 x number of variables) with function tolerance of 1e-4 and constraint tolerance of 1e-3. The results show the effectiveness of the MOGA in dealing with the in-hand problem. An evidence is the 200-20-10000 case study with end condition of "O" in which two potential solutions with the same thickness, but different structural architectures are found and reported by the platform successfully.

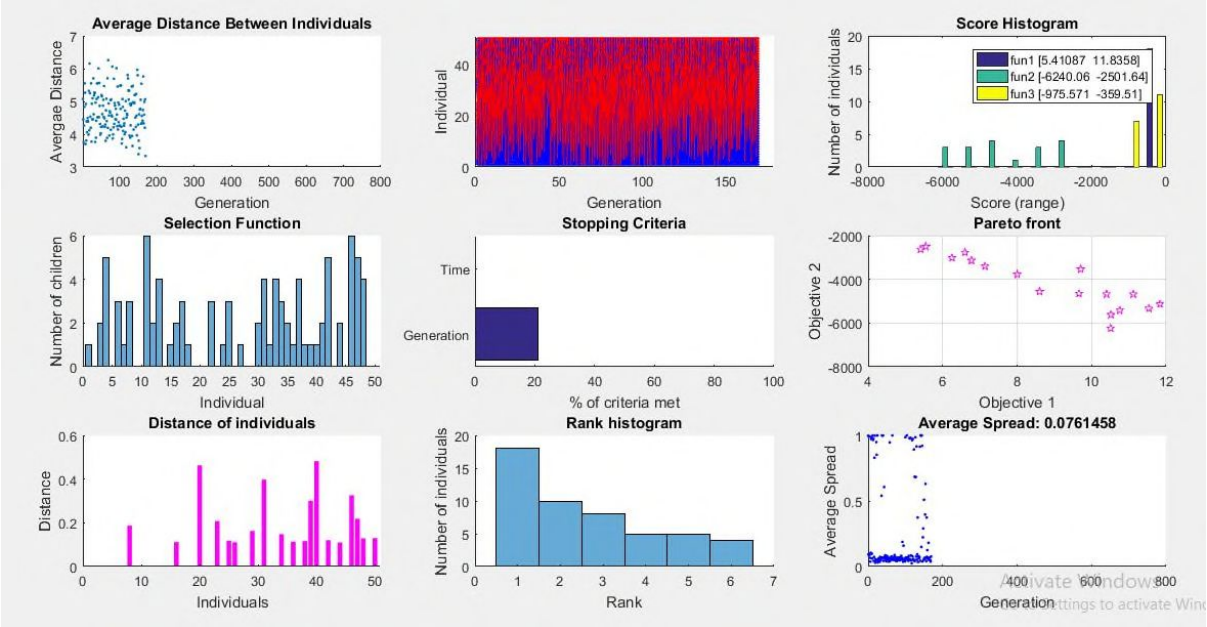

Fig. 6: A sample of the level 1 MOGA results

As it has been explained before, after accomplishment of level 1, no layer will be added or removed from the obtained lay-up configuration. But instead, the total thickness is kept unchanged and then by changing the lay-up sequence, different pipe stiffness classes are achieved and among them the very specific lay-up leading to maximum pipe stiffness class is chosen. As it is evident from Eqs. (2) to (5), pipe stiffness depends on the lay-up sequence. This is the main reason that at level 2, direct search method is employed to search among all

possible alternatives. For instance, for the case of {375-32-4000} as the output of the level one it is reported that combination of five helical layers (±62.5°) with two hoop layers will be led to the minimum thickness (i.e. 4.8 mm) and maximums for both HTS and LTS. Then at the level 2, all possible permutations for lay-up configurations with aforementioned five helical (q=5) and two hoop layers (p=2) are generated and corresponding pipe stiffness classes are calculated for all 21 cases ($\frac{(5+2)!}{5!\times 2!} = 21$). For this specific case, pipe stiffness varies from 3329 to 4896 Pa. Among 21 alternatives, maximum pipe stiffness is associated with the lay-up configuration of [90/±62.5$_5$/90] and the minimum is associated with [±62.5$_3$/90$_2$/±62.5$_2$] lay-up configuration. Thus, without changing the thickness of the pipe and just by changing the lay-up sequence, maximum value for pipe stiffness is achieved.

6. Conclusion

An integrated design and optimization process is developed to obtain the optimal structural design for FRP pipes utilized in the market of oil and gas with minimum cost. The design constraints dictated by normative standards from both short-term and long-term service viewpoints are identified. Then, appropriate computational tools are developed for estimating the identified constraints for FRP pipes based on their lay-up configurations. Extensive experimental study is conducted on the industrial-scale FRP pipes to validate the proper performance of the optimization foundation.

Then, the optimization framework is constructed by defining the minimum price and the maximum load bearing capacities from different aspects as the main objectives and design requirements and also filament winding limitations as constraints. Design variables consist of number of layers, lay-up sequence and winding angle. For this purpose, OPTICOPIPE® software is developed implementing the multi-objective optimization on two levels. At the first level, pipe thickness is minimized while strengths along circumferential and axial directions are maximized and on the second level pipe stiffness is also maximized. Genetic algorithm technique is combined with direct search in OPTICOPIPE®. Thanks to meta-heuristic optimization technique, OPTICOPIPE® is just in need of the pipe diameter, pressure class and stiffness class and also mechanical properties of the fiber and resin as input data by the user. The results obtained from the optimization platform confirms the effectiveness of the proposed methodology in dealing with the design problem. The exploration and exploitation of the solution space is being carried out by the evolutionary optimization operators and an original permutation-based direct search approach respectively. The advantage of the OPTICOPIPE® is

twofold: Very short required runtime and no dependency to the KOE in the form design background or previous experience.

Appendix A: Failure criteria and ply-discount rules for PDM

Hashin failure criteria are expressed as below [39]:

$$\left(\frac{\sigma_X}{X_T}\right)^2 + \left(\frac{\sigma_S}{S}\right)^2 \leq 1 \quad \text{(A1)}$$

$$\frac{\sigma_X}{X_C} \leq 1 \quad \text{(A2)}$$

$$\left(\frac{\sigma_Y}{Y_T}\right)^2 + \left(\frac{\sigma_S}{S}\right)^2 \leq 1 \quad \text{(A3)}$$

$$\left(\frac{\sigma_Y}{Y_C}\right)^2 + \left(\frac{\sigma_S}{S}\right)^2 \leq 1 \quad \text{(A4)}$$

$$\left(\frac{\sigma_X}{X_C}\right)^2 + \left(\frac{\sigma_S}{S}\right)^2 \leq 1 \quad \text{(A5)}$$

where abovementioned Eqs. (A1) to (A5) are associated fiber breakage, fiber compression, matrix tension, matrix compression and fiber/matrix shearing modes of failure, respectively. After occurrence of failure, material properties of the failed ply are reduced based on experienced failure mode in accordance with following degradation rules [41]:

$$(E_X, E_Y, \vartheta_X, E_S, X_T, X_c, Y_T, Y_C, S)_{intact} \rightarrow (0,0,0,0,0,0,0,0,0)_{failed} \quad \text{(A6)}$$

$$(E_X, E_Y, \vartheta_X, E_S, X_T, X_c, Y_T, Y_C, S)_{intact} \rightarrow (0,0,0,0,0,0,0,0,0)_{failed} \quad \text{(A7)}$$

$$(E_X, E_Y, \vartheta_X, E_S, X_T, X_c, Y_T, Y_C, S)_{intact} \rightarrow (E_X, 0.1E_Y, 0.1\vartheta_X, 0.1E_S, X_T, X_c, 0, Y_C, S)_{failed} \quad \text{(A8)}$$

$$(E_X, E_Y, \vartheta_X, E_S, X_T, X_c, Y_T, Y_C, S)_{intact} \rightarrow (E_X, 0.1E_Y, 0.1\vartheta_X, 0.1E_S, X_T, X_c, Y_T, 0, S)_{failed} \quad \text{(A9)}$$

$$(E_X, E_Y, \vartheta_X, E_S, X_T, X_c, Y_T, Y_C, S)_{intact} \rightarrow (E_X, E_Y, 0.1\vartheta_X, 0.1E_S, X_T, X_c, Y_T, Y_C, 0)_{failed} \quad \text{(A10)}$$

Eqs. (A6) and (A7) correspond with fiber tension and compression failure modes. Eqs. (A8), (A9) and A(10) are associated with matrix tension, matrix compression and fiber/matrix shearing modes of failure, respectively.

Appendix B: Calculating geometrical and mechanical properties of plies

The thickness of each hoop layer is calculated using below formulation:

$$t_{Hoop} = \frac{\rho_A^H}{\rho_{FRP} \times W_f} \tag{B1}$$

where W_f, ρ_A^H and ρ_{FRP} are, areal density of the hoop layer and density of composites, respectively. These parameters are calculated as below:

$$\rho_A^H = \frac{N_S T}{B} \tag{B2}$$

$$\rho_{FRP} = (V_f \rho_f + V_m \rho_m) \tag{B3}$$

$$W_f = \frac{V_f \rho_f}{V_f \rho_f + V_m \rho_m} \tag{B4}$$

the thickness of cross layers is calculated as below:

$$t_{Cross} = \frac{2 \times \rho_A^C}{\rho_{FRP} \times W_f} \tag{B5}$$

$$\rho_A^C = \frac{N_S T}{B sin\theta} \tag{B6}$$

Finally, the thickness of the structural layers is obtained as below:

$$t_r = p.t_{Hoop} + q.t_{Cross} \tag{B7}$$

Mechanical properties of each layer are obtained using below micromechanics rules [38]:

$$E_X = E_f V_f + E_m V_m \tag{B8}$$

$$\vartheta_X = \vartheta_f V_f + \vartheta_m V_m \tag{B9}$$

$$E_Y = E_m \frac{\left(1 + 2\eta_T V_f\right)}{\left(1 - \eta_T V_f\right)}; \eta_T = \frac{\frac{E_f}{E_m} - 1}{\frac{E_f}{E_m} + 2} \tag{B10}$$

$$G_{XY} = E_S = G_m \frac{(1 + \eta_T V_f)}{(1 - \eta_T V_f)}; \eta_T = \frac{\frac{G_f}{G_m} - 1}{\frac{G_f}{G_m} + 1} \tag{B11}$$

The strength components of each layer are also computed using below formulations [32, 56]:

$$X_T = X_f(V_f + V_m \frac{E_m}{E_f}) \tag{B12}$$

$$X_c = 0.5X_T \tag{B13}$$

$$Y_T = V_m X_m \tag{B14}$$

$$Y_c = V_m \acute{X}_m \tag{B15}$$

$$S = \left[1 - \left(\sqrt{V_f} - V_f\right)\right]\left(1 - \frac{G_m}{G_f}\right)S_m \tag{B16}$$

Appendix C: Mechanical properties

Mechanical properties of constituent materials utilized for manufacturing FRP pipes to investigate the accuracy level of the developed computational tools are tabulated in Table C.1.

Table C.1: Mechanical properties of glass fiber, polyester resin

Glass Fiber	Polyester resin
E_f = 78 GPa	E_m = 3.5 GPa
G_f = 32 GPa	G_m = 1.32 GPa
ν_f = 0.22	ν_m = 0.33
ρ_f = 2.56 gr/m^3	ρ_m = 1.15 gr/m^3
X_f = 2345 MPa	X_m = 78 MPa
	X'_m = 130 MPa
	S_m = 60 MPa

Acknowledgment

The authors acknowledge the financial support provided by the Iranian National Science Foundation (INSF) under contract 4003139.

Data availability statement

The datasets generated and/or analyzed during the current study are available from the corresponding author on reasonable request.

References:

[1] R. Rafiee, On the mechanical performance of Glass-Fiber-Reinforced Thermosetting-Resin pipes: A Review, Journal of Composite Structures, 2016; 143:151-164.

[2] N. J. Jin, H. G. Hwang, J. H. Yeon, Structural analysis and optimum design of GRP pipes based on properties of materials, Construction and Building Materials 2013; 38:316-326.

[3] J. H. S. Almeida Jr., M. L. Ribeiro, V. Tita, S. C. Amico, Stacking sequence optimization in composite tubes under internal pressure based on genetic algorithm accounting for progressive damage, Composite Structures 2017; 178:20-26.

[4] N. Minsch, F.H. Herrmann, T. Gereke, A. Nocke, C. Cherif, Analysis of filament winding processes and potential equipment technologies, Procedia CIRP 2017; 66: 125-130.

[5] V. Alcantar, S. Ledesma, S.M. Aceves, E. Ledesma, A. Saldana, Optimization of type III pressure vessels using genetic algorithm and simulated annealing, International Journal of Hydrogen Energy 2017; 42: 20125-20132.

[6] C. Colombo, L. Vergani, Optimization of filament winding parameters for the design of a composite pipe, Composites Part B 2018; 148: 207-216.

[7] Z. Zhang, Sh. Hou, Q. Liua, X. Hana, Winding orientation optimization design of composite tubes based on quasistatic and dynamic experiments, Thin Walled-Structures 2018; 127:425-433.

[8] C. Liu, Y. Shi, Design optimization for filament wound cylindrical composite internal pressure vessels considering process-induced residual stresses, Composite Structures 2020; 235:111755.

[9] M. H. Hajmohammad, A. Tabatabaeian, A. R. Ghasemi, F. Taheri-Behrooz A novel detailed analytical approach for determining the optimal design of FRP pressure vessels subjected to hydrostatic loading: Analytical model with experimental validation, Composites Part B 2020; 183:107732

[10] A. Khademi, A. Yousefi, M. Haghighi-Yazdi, M. Safarabadi, R. Rafiee, Numerical investigation of the effect of moisture and impurity on long-term creep behavior of polymer composite pipes, International Journal of Pressure Vessels and Piping, 2021; 193: 104456.

[11] R. Rafiee, M. Maleki, S. Rahnama, , Experimental study on the effect of hygrothermal environments combined with the sustained mechanical loads on the strength of composite rings, Composite Structures, 2021; 258: 113397

[12] R. Rafiee, A. Ghorbanhosseini, Analyzing the long-term creep behavior of composite pipes: Developing an alternative scenario of short-term multi-stage loading test, Composite Structures, 2020; 254: 112868.

[13] R. Rafiee, F. Abbasi, S. Maleki, Fatigue analysis of a composite ring: Experimental and theoretical investigations, Journal of Composite Materials, 2020; 54(26): 4011-4024.

[14] R. Rafiee, F. Abbasi, Numerical and experimental analyses of the hoop tensile strength of filament wound composite tubes, Mechanics of Composite Materials, 2020; 56(4):423-436.

[15] R. Rafiee, A. Ghorbanhosseini, Experimental and theoretical investigations of creep on a composite pipe under compressive transverse loading, Fiber and Polymers, 2021; 22(1): 222-230.

[16] R. Rafiee, A. Ghorbanhosseini, Developing a micro-macromechanical approach for evaluating long-term creep in composite cylinders, Thin-Walled Structures, 2020; 151: 106714.

[17] R. Rafiee, H. Rashedi, Sh. Rezaee, Theoretical study of failure in composite pressure vessels subjected to low-velocity impact and internal pressure, Frontiers of Structural and Civil Engineering, 2020; 14: 1349-1358.

[18] R. Rafiee, P. Sharifi, Stochastic failure analysis of composite pipes subjected to random excitation, Construction and Building Materials, 2019; 224: 950-961.

[19] R. Rafiee, A. Ghorbanhosseini, Sh. Rezaee, Theoretical and numerical analyses of composite cylinders subjected to the low velocity impact, Composite Structures, 2019; 226:111230.

[20] R. Rafiee, M. R. Habibagahi, Evaluating mechanical performance of GFRP pipes subjected to transverse loading, Thin-walled Structures, 2018; 131: 347-359.

[21] R. Rafiee, M. R. Habibagahi, On the stiffness prediction of GFRP pipes subjected to transverse loading, KSCE Journal of Civil Engineering, 2018; 22(11):4564-4572.

[22] R. Rafiee, M.A. Torabi, S. Maleki, Investigating structural failure of a filament-wound composite tube subjected to internal pressure: Experimental and theoretical evaluation, Polymer Testing, 2018; 67:322-330.

[23] S. Maleki, R. Rafiee, A. Hasannia, M. R. Habibagahi, Investigating the influence of delamination on the stiffness of composite pipes under compressive transverse loading using cohesive zone method, Frontiers of Structural and Civil Engineering, 2019; 13:1316-1323.

[24] R. Rafiee, M.A. Torabi, Stochastic prediction of burst pressure in composite pressure vessels, Composite Structures, 2018; 185:573-583.

[25] R. Rafiee, Stochastic fatigue analysis of glass fiber reinforced polymer pipes, Composite Structures, 2017; 167: 96-102.

[26] R. Rafiee, F. Eslami, Theoretical modeling of fatigue phenomenon in composite pipes, Journal of Composite Structures, 2017; 161:256-263.

[27] R. Rafiee, B. Mazhari, Evaluating long-term performance of Glass Fiber Reinforced Plastic pipes subjected to internal pressure", Construction and Building Materials, 2016; 122:694-701.

[28] R. Rafiee, B. Mazhari, Simulation of the long-term hydrostatic tests on Glass Fiber Reinforced Plastic Pipes, Journal of Composite Structures, 2016; 136:56-63.

[29] R. Rafiee, M. Fakoor, H. Hesamsadat, The influence of production inconsistencies on the functional failure of GRP pipes, Steel & Composite Structures, An International Journal, 2015; 19(6): 1369-1379.

[30] R. Rafiee, F. Reshadi, S. Eidi, Stochastic analysis of functional failure pressures in glass fiber reinforced polyester pipes, Materials & Design, 2015; 67: 422-427.

[31] R. Rafiee, F. Reshadi, Simulation of functional failure in GRP mortar pipes, Journal of Composite Structures, 2014; 113:155-163.

[32] R. Rafiee, A. Amini, Modeling and experimental evaluation of functional failure pressures in glass fiber reinforced pipes, Journal of Computational Materials Science, 2015; 96: 579-588.

[33] R. Rafiee, Apparent hoop tensile strength prediction of GRP pipes, Journal of Composite Materials 2013, 47 (11): 1377-1386.

[34] R. Rafiee, Experimental and theoretical investigations on the failure of filament wound GRP pipes, Journal of Composites Part B 2012, 45(1): 257-267.

[35] ISO 14692, Standard: petroleum and natural gas industries - glass-reinforced plastics (GRP) piping. Part 1: vocabulary, symbols, applications and materials; Part 2: qualification and manufacture; Part 3: system design; Part 4: fabrication, installation and operation 2017.

[36] ASTM D2105-01, "Standard test method for longitudinal tensile properties of fiberglass (Glass fiber reinforced thermosetting resin) pipe and tube", American society for testing and materials, 2001

[37] ASTM D2290-00, “Standard test method for apparent hoop tensile strength of plastic or reinforced plastic pipe by split disc method", American society for testing and materials, 2000.

[38] R. F. Gibson, Principles of composite material mechanics, second ed., CRC press, 2007.

[39] Z. Hashin, Failure criteria for unidirectional fiber composites, Applied Mechanics 1980: 47(2); 329-334.

[40] W. David, Progressive Failure Analysis Methodology for Laminated Composite Structure, Langley Research Center, NASA; 1999.

[41] J. H. S. Almeida Jr., M. L. Ribeiro, V. Tita, S. C. Amico, Damage and failure in carbon/epoxy filament wound composite tubes under external pressure: Experimental and numerical approaches, Materials and Design 2016; 96: 431-438.

[42] ASTM D1599-99, “Standard test method for resistance to short-time hydraulic pressure of plastic pipes, tubing, and fittings”, American society for testing and materials, 1999.

[43] ASTM D2412-02, "Standard test method for determination of external loading characteristics of plastic pipe by parallel-plate loading", American society for testing and materials, 2002.

[44] ASTM D3171-15, “Standard test method for constituent content of composite materials”, American society for testing and materials, 2015.

[45] S. Jafari, T. Nikolaidis, Meta-heuristic global optimization algorithms for aircraft engines modelling and controller design; A review, research challenges, and exploring the future. Progress in Aerospace Sciences, 2019; 104:40-53.

[46] I. Giagkiozis, R. C. Purshouse, P. J. Fleming, An overview of population-based algorithms for multi-objective optimisation. International Journal of Systems Science, 2015; 46(9):1572-99.

[47] L. I. Yinfeng, S. Jafari, T. Nikolaidis, Advanced optimization of gas turbine aero-engine transient performance using linkage-learning genetic algorithm: Part II, optimization in flight mission and controller gains correlation development, Chinese Journal of Aeronautics, 2021; 34(4):568-88.

[48] M. Affenzeller, A. Beham, S. Vonolfen, E. Pitzer, S. M. Winkler, S. Hutterer, M. Kommenda, M. Kofler, G. Kronberger, S. Wagner, Simulation-based optimization with HeuristicLab: practical guidelines and real-world applications, In Applied simulation and optimization 2015 (pp. 3-38). Springer, Cham.

[49] M. Montazeri-Gh, S. Jafari, Evolutionary optimization for gain tuning of jet engine min-max fuel controller, Journal of Propulsion and Power, 2011; 27(5): 1015-1023

[50] C. M. Fonseca, P. J. Fleming, Genetic algorithms for multiobjective pptimization: Formulation discussion and generalization. InIcga 1993 Jul 17 (Vol. 93, No. July, pp. 416-423).

[51] Y. Shan, L. Yang, Fast and frugal heuristics and naturalistic decision making: a review of their commonalities and differences, Thinking & Reasoning, 2017; 23(1):10-32.

[52] A. Safari, H. G, Lemu, S. Jafari, M. Assadi, A comparative analysis of nature-inspired optimization approaches to 2D geometric modelling for turbomachinery applications, Mathematical Problems in Engineering, 2013; Article ID 716237

[53] M. Birattari, Tuning Metaheuristics: A Machine Learning Perspective, Studies in Computational Intelligence ISSN 1860949X, DOI 10.1007/978-3-642-00483-4, First edition 2005. Second printing 2009

[54] D. K. Roylance, Netting analysis for filament-wound pressure vessels, Technical note, Composites division, Army materials and mechanics research center, Watertown, Massachusetts; 1976.

[55] R. Kumar, P. Rockett, Improved sampling of the pareto-front in multiobjective genetic optimizations by steady-state evolution: a Pareto converging genetic algorithm, Evolutionary Computation, 10 (3). pp. 283-314. ISSN 1063-6560, 2002.

[56] C. C. Chamis, Simplified composite micromechanics equations for strength, fracture toughness and environmental effects. Cleveland, Ohio, USA: NASA, Lewis Research Center; 1984. Technical Memorandum N84–27832.

Filament wound pipes optimization platform development: a methodological approach

Rafiee, Roham

2022-07-13

Rafiee R, Shahzadi R, Jafari S. (2022) Filament wound pipes optimization platform development: a methodological approach. Composite Structures, Volume 297, October 2022, Article number 115972

https://doi.org/10.1016/j.compstruct.2022.115972